JOURNAL OF BACTERIOLOGY, June 2002, p. 3176–3185 Vol. 184, No. 12
0021-9193/02/$04.00+0 DOI: 10.1128/JBA.184.12.3176–3185.2002

Atypical Processing in Domain III of 23S rRNA of *Rhizobium leguminosarum* ATCC 10004^T at a Position Homologous to an rRNA Fragmentation Site in Protozoa

Franziska Klein, Regina Samorski, Gabriele Klug, and Elena Evguenieva-Hackenberg*

Institut für Mikrobiologie und Molekularbiologie der Justus-Liebig-Universität Giessen, 35392 Giessen, Germany

Received 27 August 2001/Accepted 8 March 2002

For still unknown reasons, the 23S rRNA of many α-Proteobacteria shows a unique fragmentation pattern compared to other bacteria. The 23S rRNA processing involves RNase III and additional, yet unidentified enzymes. The α-proteobacterium *Rhizobium leguminosarum* ATCC 10004^T possesses two fragmentation sites in its 23S rRNA. The first one harbors an intervening sequence in helix 9 which is cleaved by RNase III. We demonstrate that the mature 5′ end of the resulting 2.6-kb rRNA fragment is generated by additional removal of helix 10. A fraction of the 2.6-kb rRNA is further processed in domain III, giving rise to two 1.3-kb rRNA fragments. We mapped the domain III fragmentation site and found it to be at a position which has only been reported for trypanosomatid protozoa. This fragmentation site is also unique in that it lacks an intervening sequence. We found that the simultaneous occurrence of 2.6-kb and 1.3-kb rRNA fragments is not due to interoperonal sequence differences but rather reflects slow processing. The different characteristics of the two fragmentation sites in the 23S rRNA suggest that they are processed by different mechanisms. Interestingly, the amount of 2.6-kb rRNA varies during culture growth. We observed a transient increase in the relative amount of 2.6-kb rRNA fragments during the first hours after inoculation, which points to changes in the ratio of rRNA synthesis rate to domain III processing rate during the growth of a culture.

Fragmentation of the RNA of the large ribosomal subunit has been described in many eukaryotic and prokaryotic organisms (5, 8, 9, 10, 11, 19, 24, 27–29, 32, 34). All 23S rRNA processing sites identified in Eubacteria (summarized in references 9 and 28) have until now been located at positions phylogenetically identical to rRNA fragmentation sites found in Eucarya (10, 11). This fact raises questions about the origin and evolution of the rRNA genes, and about the physiological implications of rRNA fragmentation. Additionally, the exact knowledge of the primary and secondary structure of the mature 23S rRNA fragments is important since 23S rRNA sequences are used as phylogenetic markers and for strain identification (6, 16, 30, 31).

The 23S rRNA of *Rhizobium leguminosarum* ATCC 10004^T possesses two processing sites (Fig. 1). The first one is at a position common to many α-proteobacterial species, in helix 9 of 23S rRNA. The helix 9 of *R. leguminosarum* contains an intervening sequence (IVS) (29) which is removed by RNase III cleavage (9). The 23S rRNA processing in this region leads to the occurrence of a short 5′ rRNA fragment with a length of approximately 130 nucleotides and a 3′ rRNA fragment with 2.6-kb length (27). Recently it has been shown that in *Rhodopseudomonas palustris* the RNase III cleavage of the IVS in helix 9 represents only an initial event of subsequent efficient processing steps leading to the removal of helix 10 and production of a 5.8S-like rRNA (34).

The second processing site in 23S rRNA of *R. leguminosarum* ATCC 10004^T is located in the central region of the 2.6-kb rRNA fragment, in domain III of 23S rRNA. This kind of 23S rRNA fragmentation was found in most of the studied *Agrobacterium* strains and in many *R. leguminosarum* and *R. etli* strains (27, 29). Only a fraction of the 2.6-kb rRNA fragment is processed in this region, generating two 1.3-kb rRNA fragments (Fig. 1) (27). The exact fragmentation site, the extent of the eventually removed sequences, and the reason for the simultaneous occurrence of 2.6-kb and 1.3-kb rRNA fragments in cells are not known. The central fragmentation of 23S rRNA occurs without involvement of an IVS (29), an unprecedented case among the known 23S rRNA processing events.

Although rRNA fragmentation occurs in many bacteria, its physiological importance is not clear. *Salmonella* strains with highly fragmented 23S rRNAs degrade the rRNA fragments faster than strains with less fragmented 23S rRNA as the cells enter the stationary phase (14). It was proposed that fragmented 23S rRNA provides some selective advantage to cells. On the other hand, it was shown that RNase III-deficient strains of *R. capsulatus* and *Salmonella enterica* serovar Typhimurium can grow despite the presence of unprocessed IVSs in their 23S rRNA (15, 17). Even *Escherichia coli* cells containing processed and unprocessed intervening sequences from *S. enterica* serovar Typhimurium are able to grow normally (12). Therefore it was concluded that the occurrence of IVSs and 23S rRNA fragmentation are phenotypically silent.

Members of the *Rhizobiaceae* family are of great agricultural importance and are among the most intensively studied bacteria. Nevertheless, the processing mechanisms leading to fragmentation of their 23S rRNA and the structural organization of the mature rRNA fragments are still not well understood. The aim of this work was to analyze the 23S rRNA fragmentation sites in the *R. leguminosarum* type strain, providing data

* Corresponding author. Mailing address: Institut für Mikrobiologie und Molekularbiologie der Justus-Liebig-Universität Giessen, Heinrich-Buff-Ring 26-32, 35392 Giessen, Germany. Phone: 49 641 99 35550/57. Fax: 49 641 99 35549. E-mail: Elena.Evguenieva-Hackenberg@mikro.bio.uni-giessen.de.

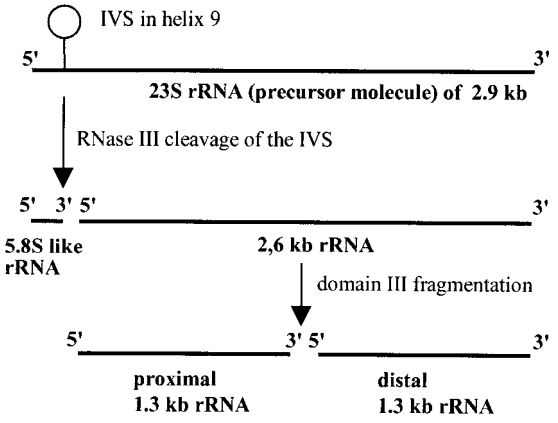

FIG. 1. Schematic representation of 23S rRNA fragmentation in *R. leguminosarum* ATCC 10004^T.

useful for understanding of the processing steps and their physiological implications, as well as for further phylogenetic and identification purposes. We demonstrate that the relative amount of 2.6-kb rRNA fragments changes during culture growth. We have localized the unique fragmentation site in the domain III of 23S rRNA at a position which has not been described before for bacteria. The characteristics of this new processing site as well as the changes in the ratio of 2.6-kb and 1.3-kb rRNAs during culture growth suggest that the domain III fragmentation is performed through a mechanism which differs from the previously described 23S rRNA processing events.

MATERIALS AND METHODS

Bacterial strains and culture conditions. The rhizobial strains *R. leguminosarum* ATCC 10004^T (USDA 2370) and *Rhizobium giardinii* H152 (1) were grown on tryptic yeast (TY) medium (3). A 50-ml TY was inoculated with *R. leguminosarum* from a plate, grown in a 100-ml flask for 36 h at 32°C and 140 rpm, and then used immediately for inoculation of large-scale cultures or kept at 4°C. Large scale semiaerobic culture consisted of 300 ml of TY in a 500-ml flask, inoculated with 30 ml of that culture, and shaken for 50 h as already described. For aerobic growth, 200 ml of TY was appropriately inoculated and incubated in a 1-liter flask.

Escherichia coli strain JM 109 (Stratagene) was grown on standard I medium (Difco).

Oligonucleotides (primers). For PCR amplification of the region between positions 109 and 205 of *R leguminosarum* ATCC 10004^T 23S rDNA (helix 9 region; *E. coli* numbering), the primers 23S-IVS-sense (23S rDNA positions 109 to 130) and 23S-IVS-antisense (23S rDNA positions 185 to 205) were used (9). The 23S rDNA region between positions 1334 and 1623 (domain III region; *E. coli* numbering) was amplified using the primers 23S-DIII-se [5′-GGGGGGAATTCTAATACGACTCACTATAG(C,T)AGGGT(T,G,A)AG(C,T)CG(G,A)CCCCTAAG(G,A)CGAGGC-3′, *Eco*RI restriction site underlined, T7 promoter region for transcription initiation in bold letters; corresponds to 23S rDNA positions 1334 to 1362] and 23S-DIII-as (5′-GGGGAAGCTTCCACCTGTGTCGGTTT[G,C,A]GG-3′; *Hin*dIII restriction site underlined; corresponds to 23S rDNA positions 1605 to 1623).

The oligonucleotide Rleg-IVS-2 (5′-ACCTGTTTTGTCCTCACGGCC-3′) was used for mapping the cleavage sites of RNase III on the left side of helix 9 of 23S rRNA. Two additional domain III sense primers were used for RNase protection analysis: 23S-DIII-se2 [5′-GGGGGAATTCG(C,T)AGGGT(T,G,A)AG(C,T)CG(G,A)CCCCTAAG(G,A)CGAG-GC-3′; *Eco*RI restriction site underlined] and DIIIse2-SQ [5′-CG(C,T)AGGGT(T,G,A)AG(C,T)CG(G,A)CCCCTAAG(G,A)CGAGGC-3′)]. The oligonucleotides 23S-DIII-int1 (5′-CCGCTCCGCTGCCCATC-3′) and 23S-DIII-int2 (5′-GGAGCTATTTCCTGGTT-3′) were used as probes in Northern hybridization experiments and are complementary to 23S rRNA regions immediately upstream of the determined 5′ end arising after domain III processing (see Fig. 3C and 3E).

All oligonucleotides were synthesized on a 380B DNA synthesizer (Applied Biosystems) or purchased from Roth (Karlsruhe, Germany).

Isolation, amplification, and analysis of nucleic acids. Total DNA was isolated according to the method of Ausubel et al. (2). Plasmids were purified with Qiagen-tip 100 columns. Cloning of PCR-amplified 23S ribosomal DNA (rDNA) regions into pUC18 or pBluescript vectors and restriction analysis were performed according to Sambrook et al. (26). Southern hybridization with digoxigenin-labeled probes was performed following the hybridization manual (Boehringer).

For rRNA quantification, *R. leguminosarum* cells were collected at certain points of the growth curve, and total RNA was isolated using the hot phenol method (33) or RNeasy columns (Qiagen). Intact ribosomes were isolated in sucrose gradient by ultracentrifugation (34); 10 μg RNA per lane was electrophoresed, blotted, and hybridized with radioactively labeled oligonucleotides (7, 13). The intensity of the obtained signals was quantified using a Molecular Imager and Quantity One software (Bio-Rad).

PCR was carried out in a final volume of 50 μl with 200 ng of total DNA as the template, using 0.8 U of *Taq* DNA polymerase (Promega) at an annealing temperature of 42°C (45 s), followed by extension at 72°C (30 s). Cycles were repeated 35 times. The resulting PCR products were purified from 3.5% small DNA low-melt agarose gels (FMC-Biozym).

Digoxigenin-labeled probes were obtained by replacing one third of the dNTP amount in a PCR with digoxigenin DNA labeling mixture (digoxigenin DNA labeling and detection kit; Boehringer).

Aliquots of 10 pmol of primer were labeled for 30 to 60 min at 37°C with 20 μCi of [γ-^{32}P]ATP using polynucleotide kinase (NEB) and subsequently purified with a NucTrap push column (Stratagene).

RNA secondary structure models were obtained online using the folding program MFOLD (18, 36).

Cell extract from *R. leguminosarum*. Cells from a 1.5-ml *R. leguminosarum* culture (exponential growth phase) were resuspended and sonified in 200 μl of extraction buffer containing 50 mM Tris-HCl (pH 7.9), 0.25 M KCl, 2 mM EDTA, 1 mM β-mercaptoethanol, 0.1 mM dithiothreitol (DTT), and 0.5 mM phenylmethylsulfonyl fluoride (PMSF) (25). The extract was centrifuged for 5 min at 10,000 × *g*, and the supernatant was used for enzymatic tests.

In vitro transcription of RNA and RNase III activity assays. In vitro transcriptions were performed adding 0.2 μg of PCR-amplified 23S rDNA region directly in a 20-μl final reaction volume containing 0.5 mM each of the rNTPs, 75 U of T7 polymerase, and the supplied T7 buffer (NEB). Alternatively, cloned 23S rDNA regions under the control of a T7 promoter were transcribed in vitro after plasmid linearization. In this case, 1 μg of DNA was used as the template. After incubation for 2 h at 37°C, the reaction mixture was phenol extracted, ethanol precipitated, and dissolved in 50 μl of water. RNase III cleavage assays were performed as previously described (7). Briefly, 1 μl (150 to 200 nM) of transcript was incubated with purified RNase III (60 nM dimer) or 2 μl of cell extract in cleavage buffer (30 mM Tris-HCl, pH 7.5, 10 mM $MgCl_2$, 130 mM KCl, 5% glycerol) for 5 min at 37°C. After phenol extraction and ethanol precipitation, the processed RNA was used for primer extension reactions.

Mapping of RNA 5′ ends by primer extension. To determine the exact RNase III cleavage positions in helix 9 of 23S rRNA and the mature 5′ end of the 2.6-kb rRNA fragment in vivo, we performed primer extension analysis with the radioactively labeled 23S-IVS-antisense and Rleg-IVS-2 primers. As templates, total RNA or in vitro processed transcripts were used. The mature 5′ end of the distal 1.3-kb rRNA fragment was determined using the 23S-DIII-as primer and total RNA.

For the primer extension reactions, 2 μg of RNA was vacuum dried and dissolved in 5 μl of 2× primer extension buffer (100 mM Tris-HCl, pH 8.3, 100 mM KCl, 20 mM $MgCl_2$, 20 mM DTT, 0.2 mM spermidine, 2 mM each of the deoxynucleoside triphosphates [dNTPs]). Approximately 80,000 cpm of primer and 5 μg of yeast tRNA were added, and the samples were incubated in a 10-μl final volume for 2 min at 95°C and 10 min at 70°C and cooled to room temperature. Another 5 μl of 2× primer extension buffer, 1.4 μl of 40 mM sodium pyrophosphate, 2.6 μl of water and 1 μl of avian myeloblastosis virus (AMV) reverse transcriptase (10 U/μl) were added, and the reaction mixtures were incubated for 30 min at 42°C. The samples were ethanol precipitated, and aliquots were analyzed on a polyacrylamide-urea gel. [α-^{35}S]dATP-labeled sequencing reactions (T7 Sequencing Kit; Pharmacia Biotech) of the cloned DNA template were loaded on the same gel to map the positions of the primer extension signals.

Mapping of RNA 3′ ends by RNase protection analysis. RNA 3′ ends occurring after domain III processing were mapped using the RNase protection assay

kit (HybSpeed RPA; Ambion). For this purpose, the analyzed domain III region was amplified using the primers 23S-DIII-se2 and 23S-DIII-as and cloned in pBluescript which was cut with *Eco*RI and *Hin*dIII. After linearization of the construct with *Eco*RI, radioactively labeled antisense RNA (RNase protection probe) was synthesized; 100,000 cpm of antisense RNA and 5 μg of total RNA were coprecipitated, denatured, hybridized, and treated with RNases as described by the manufacturer. [α-^{35}S]dATP-labeled sequencing reactions (T7 Sequencing Kit; Pharmacia Biotech) of the cloned DNA template were loaded on the same gel to map the positions of the signals. The sequencing primer used was DIIIse2-SQ.

RESULTS

Helix 10 is removed in addition to helix 9 during the 5′-end processing of 23S rRNA in *R. leguminosarum*. 23S rRNA of *R. leguminosarum* is processed near its 5′ end, leading to the occurrence of a small rRNA of approximately 130 nucleotides and a large 2.6-kb rRNA. This fragmentation is due to the processing of an IVS in helix 9 (29) (Fig. 1). The locations of the 5′ ends generated during this processing are yet not known.

It was reported that in some α-Proteobacteria, in addition to the RNase III cleavage in helix 9, helix 10 processing by an unknown enzyme(s) creates the 5′ end of the 2.6-kb rRNA fragment (9, 34, 35). This prompted us to examine the extent of 23S rRNA sequences removed during the processing in the helix 9 region of *R. leguminosarum*.

The 5′ ends arising during this processing were mapped by primer extension analysis. Since neither the RNase III protein nor the *rnc* gene has been identified in *Rhizobium* spp., we used purified RNase III from *R. capsulatus* (Rc-RNase III) and *E. coli* (Ec-RNase III) in order to localize the RNase III processing region in the IVS. The primer extension analysis was performed with RNase III-processed in vitro transcript containing helices 8, 9, and 10 of *R. leguminosarum* ATCC 10004^T 23S rRNA (Fig. 2A; comprises the 23S rRNA sequences between positions 109 and 205, *E. coli* numbering). To distinguish the signals representing the 5′ ends of RNA fragments from those arising due to structural obstacles leading to a premature end of the reverse transcriptase reaction, we included the unprocessed in vitro transcript as a control in the primer extension reactions. In vivo 5′ ends were localized by primer extension analysis of total RNA from *R. leguminosarum* ATCC 10004^T.

The scissile bonds on the left side of helix 9 were mapped using the primer Rleg-IVS-2 (shown in Fig. 2A). The signals obtained by primer extension are presented in Fig. 2B, and the positions of the RNase III cleavages are marked by arrows in Fig. 2A. The major signals are located in the RNA sequence region 5′-AAUCUGUU-3′. The in vivo 5′ end corresponds to RNase III processing at the U/G site (Fig. 2B, lane 2). Rc-RNase III also cleaves at the U/G site and two nucleotides upstream, at the U/C position (Fig. 2B, lane 3). Ec-RNase III processes only the U/C bond in this RNA region (Fig. 2B, lane 4). The same bond was also cleaved in vitro by an enzymatic activity from *R. leguminosarum* cell extracts, most probably representing the endogenous RNase III (not shown). Thus, the RNase III of three different bacterial species recognizes the same RNA region and efficiently uses at least one of the two possible scissile bonds. We observed signals of lower intensity upstream (Fig. 2B, lane 2) and downstream (lanes 2, 3, and 4) of the major signals. They may represent secondary RNase III cleavage sites.

The RNase III cleavage sites on the right side of helix 9 were mapped using the primer 23S-IVS-antisense (Fig. 2A). The signals obtained by primer extension are presented in Fig. 2C, and the positions of RNase III cleavage are marked by arrows in Fig. 2A. All cleavage sites were localized in the region 5′-UUUCUAGG-3′. Rc-RNase III cleaves at three sites, and the intensity of the signals suggests a preference for the two downstream scissile bonds, 5′-UU/UC/UA/GG-3′ (Fig. 2C, lane 1). Ec-RNase III prefers the C/U processing site (Fig. 2C, lane 2). In addition, we found that Ec-RNase III cleaves the A/G site. An enzymatic activity from *R. leguminosarum*, most probably representing the endogenous Rl-RNase III, processed the in vitro transcript at the scissile bond U/U, the most upstream cleavage site used by Rc-RNase III (compare lanes 1 and 3 in Fig. 2C). The identical cleavage site was also detected in vivo, in a primer extension reaction in which total RNA was used as a template (Fig. 2C, lane 4).

The RNase III-specific signal detected in vivo was very weak, suggesting additional processing at the 5′ end of the 2.6-kb rRNA fragment. Indeed, an additional very strong signal was obtained downstream, obviously representing the mature 5′ end (Fig. 2C, lane 4). This mature 5′ end was mapped 10 nucleotides upstream of the 3′ end of the antisense primer used, at the base of helix 10 (marked M in Fig. 2A). Sequencing reactions of templates with known sequences were used as a nucleotide ladder (not shown). Thus, in addition to the RNase III cleavage of the IVS in helix 9, further processing events remove the helix 10 sequences from the primary 23S rRNA transcript in *R. leguminosarum*, as in other α-Proteobacteria (34, 35).

It was discussed previously that the first 30 bp of the IVS-containing helix 9 of different α-Proteobacteria are relatively conserved and provide invariant helix structures as predicted by the MFOLD computing program (9). Almost all the RNase III cleavage sites map in the middle of this helix structure in *R. leguminosarum* ATCC 10004^T (Fig. 2A). The positioning of the RNase III cleavage sites relative to each other on both sides of helix 9 is unusual. The scissile bonds corresponding to the in vivo detected 5′ ends on both sides of helix 9 (Fig. 2A) are separated by five and not by two base pairs, as expected (21). The same applies for the Ec-RNase III cleavage sites (Fig. 2A). This finding may be useful for future studies on the specificity of RNase III, which is still not well understood (9, 21).

Domain III fragmentation site in 23S rRNA of *R. leguminosarum* ATCC 10004^T corresponds to an rRNA processing site in trypanosomatid protozoa. It was previously shown that the central fragmentation of the large 2.6-kb rRNA produces two 1.3-kb rRNA fragments in *R. leguminosarum* ATCC 10004^T (27) (Fig. 1). We localized the mature 5′ end of the distal 1.3-kb rRNA fragment by primer extension, using the primer 23S-DIII-as and total RNA as a template. As negative controls, unprocessed in vitro transcripts covering the investigated rRNA region and total RNA from the strain *R. giardinii* H152, which lacks 23S rRNA fragmentation in domain III, were included in the analysis (Fig. 3A). The position of the determined 5′ end is indicated with an arrow marked 5′ in Fig. 3C, which shows the putative secondary structure of the domain III region (29). This 5′ end is located at a position which has not been described earlier as an rRNA fragmentation site in bacteria and which differs from the previously proposed fragmentation site (29). Interestingly, this position corresponds to a

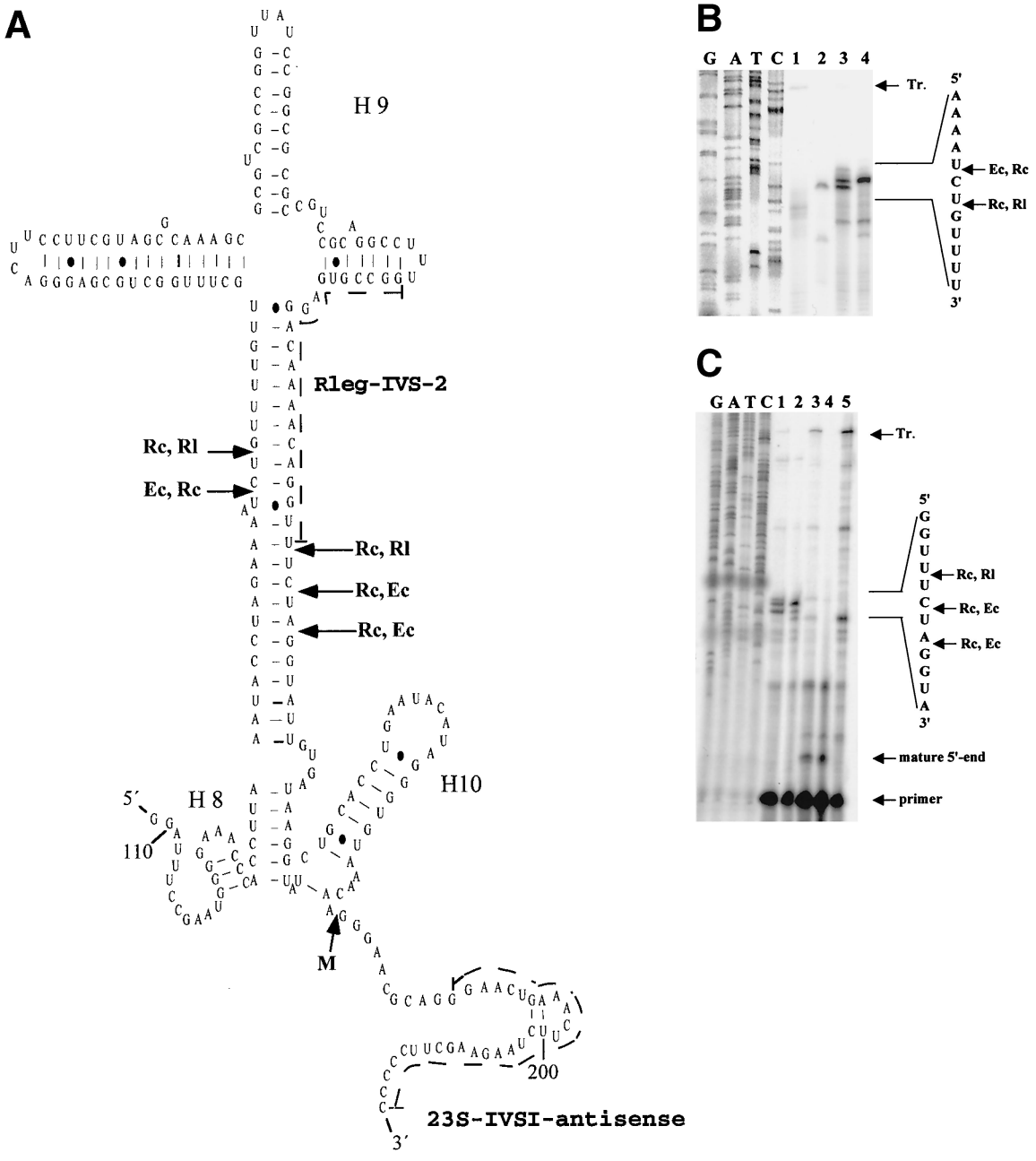

FIG. 2. Mapping of 5′ ends which occur due to processing in the region of helices 9 and 10 of 23S rRNA of *R. leguminosarum* ATCC 10004^T. (A) Model of the potential secondary structure of 23S rRNA positions 109 to 205 (*E. coli* numbering) in *R. leguminosarum* ATCC 10004^T. H8, H9, and H10, helices 8, 9, and 10, respectively. The positions of primers 23S-IVSI-antisense and Rleg-IVS-2 are marked with lines on the side of the complementary rRNA sequences. The positions of the helix 9 RNase III cleavage sites in vitro and in vivo and of the mature 5′ end of the 2.6-kb rRNA fragment in vivo, as determined by primer extension analysis, are indicated by arrows. Rc, cleavage site of Rc-RNase III in vitro; Ec, cleavage site of Ec-RNase III in vitro; Rl, cleavage site of Rl-RNase III from *R. leguminosarum*; M, mature 5′ end of the 2.6-kb rRNA fragment in vivo. (B) Determination of RNase III cleavage sites on the left side of helix 9 using primer Rleg-IVS-2. The following RNAs were used as templates in primer extension reactions: 1, unprocessed in vitro transcript; 2, *R. leguminosarum* total RNA; 3, in vitro transcript cleaved with Rc-RNase III; 4, in vitro transcript cleaved with Ec-RNase III. Lanes G, A, T, and C each refer to the corresponding nucleotide of the DNA template (cloned 23S rDNA region) as determined by sequencing. A part of the rRNA sequence is indicated on the side of the panel. The signals corresponding to the detected 5′ ends are marked by arrows (descriptions as in A). Tr., 5′ end of the unprocessed transcript. (C) Determination of RNase III cleavage sites on the right side of helix 9 using primer 23S-IVSI-antisense. The following RNAs were used as templates in primer extension reactions: 1, in vitro transcript cleaved with Rc-RNase III; 2, in vitro transcript cleaved with Ec-RNase III; 3, in vitro transcript incubated with *R. leguminosarum* cell extract; 4, *R. leguminosarum* total RNA; 5, unprocessed in vitro transcript. Lanes G, A, T, and C each refer to the corresponding nucleotide of the DNA template (cloned 23S rDNA region) as determined by sequencing. A part of the rRNA sequence is indicated on the side of the panel. The signals corresponding to the detected 5′ ends are marked by arrows (descriptions as in A). Tr., 5′ end of the unprocessed transcript.

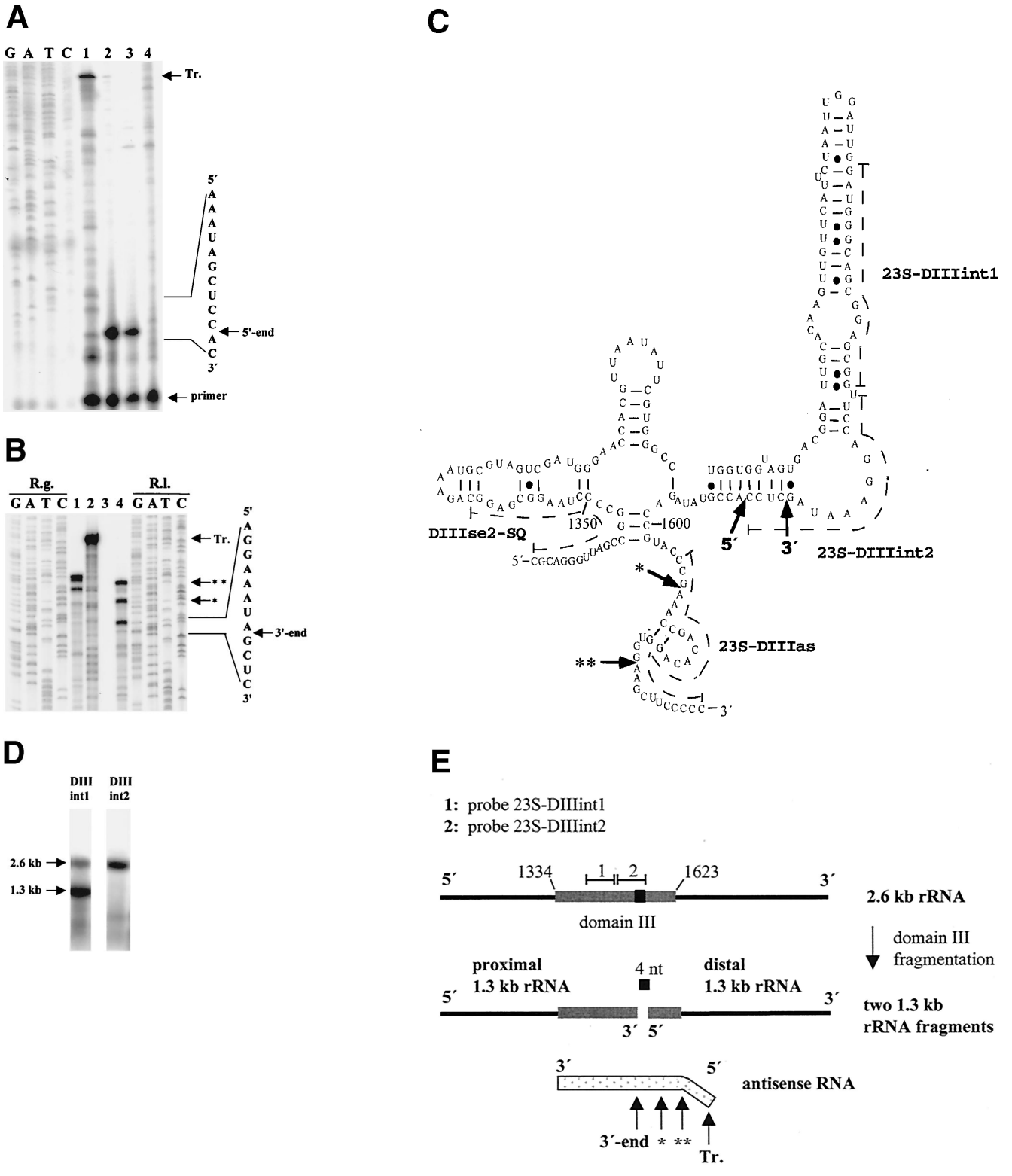

FIG. 3. Characterization of the domain III processing site of 23S rRNA in *R. leguminosarum* ATCC 10004^T. (A) Determination of the 5′ end of the distal 1.3-kb rRNA fragment via primer extension analysis. The following rRNAs were used as templates: 1, unprocessed in vitro transcript; 2 and 3, *R. leguminosarum* total RNA; 4, *R. giardinii* total RNA. Lanes G, A, T, and C each refer to the corresponding nucleotide of the DNA template (cloned 23S rDNA region) as determined by sequencing. A part of the rRNA sequence is indicated on the side of the panel. The signals corresponding to the detected 5′ end, to the unprocessed transcript (Tr.), and to the primer are marked by arrows. (B) Determination of the 3′ end of the proximal 1.3-kb rRNA fragment via RNase protection analysis. Lanes G, A, T, and C each refer to the corresponding nucleotide of the

processing site in the nucleus-encoded rRNA of the protozoa *Crithidia fasciculata*, *Trypanosoma brucei*, and *Trypanosoma cruzi* (reviewed in reference 11).

We performed RNase protection analyses in order to identify the 3′ end of the proximal 1.3-kb rRNA fragment in *R. leguminosarum* ATCC 10004^T (Fig. 3B). As the RNA protection probe, in vitro labeled antisense RNA comprising the analyzed domain III region of 23S rRNA was used (lane 2 in Fig. 3B). This probe includes approximately 50 nucleotides which are not complementary to 23S rRNA and originate from the cloning vector. Three signals were obtained in the RNase protection assay performed with total RNA of *R. leguminosarum* ATCC 10004^T (lane 4 in Fig. 3B). The signal corresponding to the most upstream nucleotide obviously represents the 3′ end of the proximal 1.3-kb rRNA fragment and was localized four nucleotides upstream of the 5′ end of the distal 1.3-kb fragment (Fig. 3C). The signal marked with two asterisks (lane 4 in Fig. 3B) is due to the hybridization of the labeled antisense RNA to the 2.6-kb rRNA present in the sample (compare with Fig. 3C and Fig. 3E). The signal marked with one asterisk corresponds to the degenerate position of the primer 23S-DIII-as used for amplification and cloning of domain III.

To exclude that this signal represents the real 3′ end of rRNA fragments, we performed Northern hybridization analysis with the oligonucleotides 23S-DIII-int1 and 23S-DIII-int2 (Fig. 3D). The probes used are shown schematically in Fig. 3C and Fig. 3E. The 23S-DIII-int1 probe hybridizes with the proximal 1.3-kb rRNA fragment as well as with the 2.6-kb rRNA, whereas the 23S-DIII-int2 probe only hybridizes with the 2.6-kb rRNA (Fig. 3D). This result shows that at least a part of the 23S-DIII-int2 target sequence is absent from the proximal 1.3-kb rRNA fragment. This finding fits well with the results from the RNase protection analysis which suggest that four nucleotides are removed during domain III processing. Three of the removed nucleotides are cytidines and one of them is a uridine. This can explain the failure of the very AT-rich 23S-DIII-int2 probe to hybridize with the proximal 1.3-kb rRNA under the stringent washing conditions used (48°C, 0.1× SSC).

The Northern hybridization shown in Fig. 3D confirms the existence of a 3′ end upstream of the 5′ end determined by primer extension analysis and excludes the possibility that an alternative domain III fragmentation position exists downstream of this 5′ end (Fig. 3C and 3E). If a fraction of the 2.6-kb rRNA was centrally fragmented at a different position downstream of that shown in Fig. 3C, the resulting proximal 1.3-kb rRNA fragments should hybridize to the 23S-DIII-int2 oligonucleotide (Fig. 3E). We conclude that the four nucleotides between the arrows shown in Fig. 3C are absent in all proximal 1.3-kb rRNA fragments.

As an additional control confirming the authenticity of the mapped 3′ end, we performed RNase protection analysis with total RNA of *R. giardinii* H152. An in vitro-labeled antisense RNA comprising the domain III region of *R. giardinii* 23S rRNA (positions 1334 to 1623, *E. coli* numbering) was used as an RNA protection probe. In accordance with the fact that this strain does not exhibit domain III fragmentation of 23S rRNA, no signal in the region corresponding to the 3′ end found in *R. leguminosarum* ATCC 10004^T was detected (compare lanes 1 and 4 in Fig. 3B). The signals detected in Fig. 3B, lane 1, map to the region of the primer 23S-DIII-as used for amplification and cloning of domain III of *R. giardinii* H152.

The mature rRNA ends arising after domain III fragmentation do not directly point to the nature of the processing enzyme(s). The involvement of RNase E is unlikely, because this enzyme preferentially cleaves AU-rich single-stranded rRNA regions (4). Since both ends map to a putative RNA helix, it cannot be excluded that the cleavage is catalyzed by a double-strand-specific endoribonuclease such as RNase III, although no IVS is present at this position and the helix is very short. We performed in vitro assays using the domain III transcript of *R. leguminosarum* (positions 1334 to 1623, *E. coli* numbering) in order to examine the involvement of RNase III. We did not detect RNase III cleavage using purified Ec- and Rc-RNase III and *R. leguminosarum* ATCC 10004^T cell extract (not shown).

We repeated the in vitro assays using a larger domain III transcript covering 23S rRNA positions 1289 to 1650 (*E. coli* numbering). The secondary structure of this transcript proposed by the MFOLD program more closely resembles the domain III secondary structure of 32 α-proteobacterial 23S rRNAs which can be found in the database. This larger transcript was also not processed endonucleolytically in vitro by either purified heterologous RNases III or cell extract (not shown). Thus, the domain III processing activity remains unidentified.

rDNA sense strand as determined by sequencing. R.g., rDNA sequence of *R. giardinii* H152; R.l., rDNA sequence of *R. leguminosarum* ATCC 10004^T; 1, total RNA of *R. giardinii* was used for hybridization with the *R. giardinii* radioactively labeled antisense RNA followed by RNase digestion; 2, *R. leguminosarum* antisense RNA (RNase protection probe) without RNase; 3, *R. leguminosarum* antisense RNA incubated with RNase in the absence of total RNA; 4, *R. leguminosarum* antisense RNA hybridized with total RNA of *R leguminosarum* and subsequently treated with RNase. A part of the rRNA sequence is indicated on the side of the panel, and the position of the mature 3′ end of the proximal 1.3-kb rRNA fragment is shown by an arrow. Additional signals arising due to the presence of 2.6-kb rRNA in the sample are marked by asterisks. Tr., full-length transcript. (C) Model of the secondary structure of the transcript comprising the analyzed domain III region of 23S rRNA in *R. leguminosarum* ATCC 10004^T (29; 23S rRNA positions 1334 to 1623, *E. coli* numbering). The positions of the mature ends arising after domain III processing, as determined by primer extension and RNase protection analysis, are indicated by arrows marked 5′ and 3′. Arrows marked with asterisks correspond to the additional signals shown in B. The positions of the oligonucleotides DIIIse2-SQ (used for the sequencing reaction loaded beside the RNase protection analysis samples), 23S-DIII-int1 and 23S-DIII-int2 (used for hybridization), and 23S-DIII-as (used for primer extension) are marked with lines on the side of the complementary rRNA sequences. (D) Northern hybridization of total RNA separated on 1.2% agarose–formaldehyde gels with oligonucleotides 23S-DIII-int1 and 23S-DIII-int2. The size of the detected 23S rRNA fragments is shown on the side of the panel. (E) Schematic diagram showing the relationship between the 2.6-kb and 1.3-kb rRNA fragments, the antisense RNA (RNase protection probe), the oligonucleotide probes 23S-DIII-int1 and 23S-DIII-int2 used for hybridization, and the positions of the signals obtained by RNase protection analysis (marked with arrows, compare with panels B and C). The antisense RNA contains at the 5′ end approximately 50 nucleotides originating from the cloning vector. The sequence complementary to rRNA starts at the position marked by two asterisks.

Only a fraction of the 2.6-kb rRNA pool is centrally fragmented despite the lack of interoperonal sequence differences in the processing region. A feature distinguishing the domain III fragmentation site from all other known 23S rRNA fragmentation sites in bacteria is the lack of an IVS in the processing region. We tested the hypothesis that domain III sequence differences between the particular *rrn* operons are responsible for the simultaneous occurrence of 2.6-kb and 1.3-kb rRNA in total RNA isolated from some strains of *Rhizobiaceae* (27). In a Southern hybridization experiment, the domain III regions of the three particular *rrn* operons of *R. leguminosarum* ATCC 10004^T were localized on *Bam*HI-generated DNA fragments with lengths of 4.2, 5.5, and 8.2 kb, respectively (not shown). DNA fragments of corresponding length were isolated from a preparative agarose gel and used as templates for PCR amplification of the separated domain III regions. The amplified regions were cloned, and plasmids from two clones corresponding to each of the *rrn* operons were sequenced. All sequences were identical to each other and to the already published sequence of this domain III region of 23S rRNA in *R. leguminosarum* ATCC 10004^T (EMBL accession number Y09784) (29). Thus, the amount of 2.6-kb rRNA molecules which are fragmented in domain III is not due to interoperonal sequence differences.

The amount of 2.6-kb rRNA species changes during culture growth. We observed an apparent decrease in the amount of the 2.6-kb rRNA in relation to the amount of 1.3-kb rRNA, when total RNA isolated at different stages of growth was separated in a formaldehyde agarose gel and stained with ethidium bromide (not shown). In order to increase the sensitivity of detection of intact 2.6-kb rRNA during late growth phases, we performed Northern hybridization. A representative Northern blot demonstrating a strong decrease in the amount of 2.6-kb rRNA during culture growth is shown in Fig. 4A. Two hours after inoculation, the cells of this culture contained more of the 2.6-kb rRNA than the 1.3-kb rRNA fragments. At later time points most of the 2.6-kb rRNA was converted into the 1.3-kb rRNA fragments. The growth curve of this particular culture during the first 24 h after inoculation is shown in Fig. 4B.

We further analyzed the changes in the relative amounts of 2.6-kb and 1.3-kb rRNA during bacterial growth, especially during the first hours after inoculation. In order to analyze the influence of different physiological conditions on the amount of 2.6-kb rRNA molecules, large-scale cultures were grown aerobically or semiaerobically. To analyze the influence of the physiological state of the inoculum on 2.6-kb rRNA amount, the large-scale cultures were inoculated either with fresh cells (grown for 36 h after inoculation of the medium from a plate and used immediately) or with old cells (half of the same inoculum kept at 4°C for 72 h). The growth behavior of the cultures is shown in Fig. 4B. The cultures inoculated with fresh cells exhibited no lag phase. In the first 8 h a high growth rate ($\mu = 6.9\ day^{-1}$) and between 8 and 24 h after inoculation a slow growth rate (average $\mu = 2.4\ day^{-1}$) were observed. The cells reached the stationary phase at about 48 h after inoculation (not shown). For the cultures inoculated with old cells, a lag phase of approximately 90 min was observed. Otherwise, all four cultures exhibited similar growth rates. The oxygen supply did not have any influence on the growth behavior (Fig. 4B).

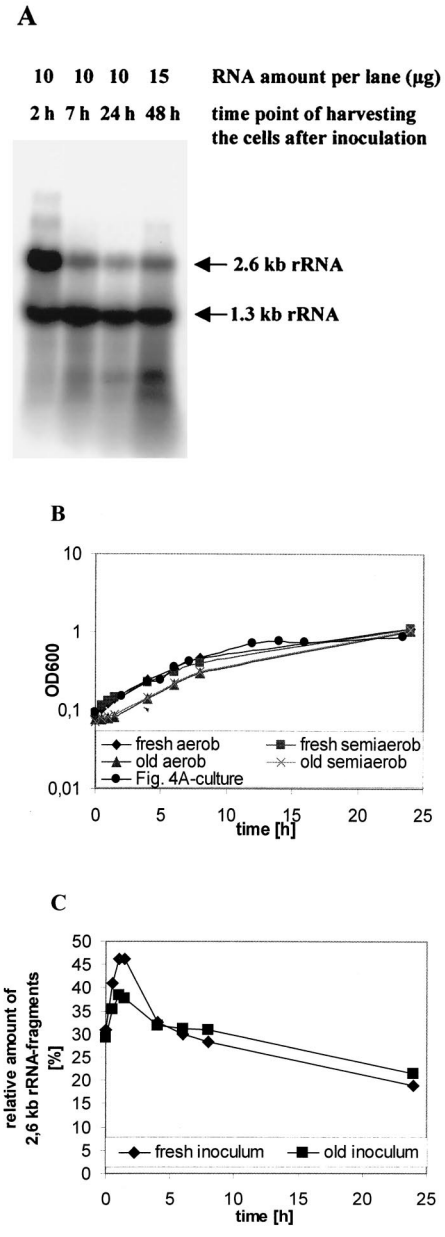

FIG. 4. Ratio of 2.6-kb to 1.3-kb rRNAs changes during growth of *R. leguminosarum* ATCC 10004^T. (A) A representative Northern hybridization of total RNA with the radioactively labeled oligonucleotide 23S-DIII-int1. The time point of harvesting the cells after inoculation of a semiaerobic culture and the amount of total RNA loaded per lane are indicated on the top of the panel. The size of the detected 23S rRNA fragments is shown on the side of the panel.(B) Growth curves of five *R. leguminosarum* cultures. One of the curves corresponds to the semiaerobic culture analyzed in A. The other four curves show the growth of semiaerobic and aerobic *R. leguminosarum* cultures inoculated with a fresh inoculum or with the same inoculum kept at 4°C for 72 h (old inoculum) and analyzed in Fig. 3C. (C) Changes in the relative amount of 2.6-kb rRNA during the growth of *R. leguminosarum* cultures inoculated with fresh or old inoculum. Northern blots were performed with total RNA using the oligonucleotides 23S-IVS-antisense and 23S-DIII-int1. At the following time points after inoculation, samples for isolation of total RNA were harvested: 30 min, 60 min, 90 min, 4 h, 6 h, 8 h, and 24 h. The curves represent the quantitative analysis of the signals obtained. The sum of the intensity of the 1.3-kb and 2.6-kb signals per each lane was defined as 100% of 23S rRNA sequences. The values did not deviate by more than 8%.

Northern blot analysis was performed with total RNA isolated at different stages of growth. In each lane, the sum of the intensity of the 1.3-kb and 2.6-kb signals was defined as 100% of 23S rRNA, and the relative amount of 2.6-kb rRNA at each time point was determined. The results are presented in Fig. 4C. In the inoculum, approximately 30% of the 23S rRNA signals originated from intact 2.6-kb rRNA. The relative amount of 2.6-kb rRNA increased during the first 90 min after inoculation to 47% for the cultures inoculated with fresh cells and to 38% for the cultures inoculated with old cells. No differences were observed between aerobically and semiaerobically grown cultures (not shown). The original value of 30% was reached 4 h after inoculation and remained relatively stable during exponential growth. In the time between 8 h and 24 h after inoculation, when growth slows down, the amount of 2.6-kb rRNA decreased to approximately 20%. The analysis of changes in the relative amounts of the different rRNA fragments was repeated using in addition oligonucleotide 23S-DIII-as as the probe, producing essentially the same results (not shown).

Surprisingly, the highest amount of 2.6-kb rRNA was reached 90 min after inoculation with fresh or with old cells despite the growth differences observed between the two types of cultures during these 90 min (Fig. 4B and C). This result suggests that both types of cultures exhibit similar temporal changes in the domain III processing rate in relation to rRNA synthesis rate. The reasons for the observed variation in the maximal amount of 2.6-kb rRNA achieved by different bacterial cultures during the early growth stages (Fig. 4C, also compare with Fig. 4A) are not known.

We tested whether 2.6-kb rRNA fragments are assembled into 50S ribosomal subunits. Isolation of ribosomes from fast-growing cells using sucrose density gradient and ultracentrifugation followed by Northern hybridization revealed that 50S subunits contain both 1.3-kb and 2.6-kb rRNAs, the latter representing approximately 20% of total 23S rRNA sequences (not shown).

DISCUSSION

We characterized the fragmentation sites in 23S rRNA of *R. leguminosarum* ATCC 10004^T. The exact RNase III cleavage sites in helix 9 of 23S RNA were localized. The in vivo 5′ end produced by RNase III cleavage on the right side of helix 9 is not easily detectable due to helix 10 processing by an yet unknown mechanism. The fragmentation in this 23S rRNA region is probably initiated by RNase III cleavage of the IVS in helix 9, and the mature 5′ end of the 2.6-kb rRNA fragment is subsequently generated by helix 10 processing. The temporal relationship of these events was previously proposed for *Rhodopseudomonas palustris* (34) and was experimentally demonstrated for *R. capsulatus* (9). No 23S rRNA processing was observed in an RNase III-deficient *R. capsulatus* mutant, showing that the failure of RNase III to cleave helix 9 also abolishes helix 10 processing in this organism. On the other hand, RNase III is not responsible for helix 10 cleavage, as shown by in vitro assays of substrates containing both helices (9, 34, 35).

The mature 5′ end of the 2.6-kb rRNA was mapped to a position similar to that described recently for *R. palustris* and *Bradyrhizobium* spp. (34, 35), suggesting that this extensive processing is a common but specific feature of α-Proteobacteria exhibiting 23S rRNA fragmentation near the 5′ end (9, 27, 28, 34, 35). The position of the internal transcribed spacer ITS2 in eukaryotic primary rRNA transcripts corresponds to the final loop in helix 10 of bacterial 23S rRNA (10, 11). After ITS2 processing, the 3′ end of 5.8S rRNA and the 5′ end of 28S rRNA form a discontinuous helix. The small rRNA fragment arising from processing in the region of helices 9 and 10 resembles eukaryotic 5.8S rRNA (Fig. 1). The rRNA structure corresponding to helix 9 of bacterial 23S rRNA is also present at the 3′ end of eukaryotic 5.8S rRNA and forms a discontinuous helix in some dipteran insects (10, 11).

The fact that helices 9 and 10 are present in all other organisms underlines their highly conserved nature. Nevertheless, they are missing in a broad group of α-Proteobacteria. Removal of other conserved structures from fragmented 23S rRNA was previously described for the α-proteobacterium *R. capsulatus*. In this case the RNase III-dependent cleavage of an IVS in helix 46 of 23S rRNA is followed by processing of the downstream sequences, which usually are part of the 23S rRNA (15). It is not known which enzymes operate in addition to RNase III during the 23S rRNA processing in α-Proteobacteria at sites harboring IVSs. The extensive processing of conserved rRNA regions during the RNase III-dependent 23S rRNA fragmentation was described until now only in α-Proteobacteria. In contrast, in *Salmonella* spp. (5) and *Spirochaeta* spp. (24), only the IVSs in helices 25 and/or 45 are removed.

We propose that additional 23S rRNA processing mechanisms operate in some α-Proteobacteria, leading to an rRNA structure which differs from that of other bacteria. The different 23S rRNA fragmentation sites found in α-Proteobacteria (in the region of helices 9 to 10, in helix 46, and in domain III) (8, 9, 15, 27, 34), compared with the fragmentation sites found in γ- and ε-Proteobacteria and in *Spirochaeta* (in helices 25 and 45) (5, 19, 24, 32) also point in the direction of different pathways in the evolution of the *rrn* genes.

The domain III fragmentation site of *R. leguminosarum* ATCC 10004^T identified in the present study represents a novel bacterial 23S rRNA processing site homologous to an rRNA fragmentation position described only in trypanosomatid protozoa (10, 11). However, it is known that discontinuities at certain variable rRNA regions do not negatively influence the function of the ribosomes (10, 11). Domain III is such a variable 23S rRNA region which in α-Proteobacteria is approximately 100 nucleotides shorter than in *E. coli* and other bacteria (16). In Eucarya, several distinct rRNA fragmentation sites in the region corresponding to domain III of 23S rRNA are known. Thus, the novel 23S rRNA processing site found in *R. leguminosarum* ATCC 10004^T represents one of the possible rRNA discontinuity positions. Interestingly, it exhibits characteristics which distinguish it from all other 23S rRNA processing sites: no IVS is found at the fragmentation site, and only a fraction of the 2.6-kb rRNA pool is centrally fragmented despite the lack of interoperonal sequence differences in the processing region.

We found that the amount of 2.6-kb rRNA changes during culture growth. A transient increase in the amount of 2.6-kb rRNA in the first hours after inoculation was reproducibly observed. It reflects an imbalance between the rate of rRNA synthesis and that of domain III processing. Nothing is known

about the regulation of these processes in *Rhizobium* spp. Nevertheless, our results suggest that the processing kinetics of the two 23S rRNA fragmentation sites in *R. leguminosarum* type strain differ markedly. The RNase III processing near the 5′ end is very fast and efficient, and therefore 23S rRNA molecules with an intact helix 9 cannot be detected by Northern blot analysis, even at the time points at which the peak of 2.6-kb rRNA amount is observed (27) (not shown). The different processing kinetics as well as the characteristics distinguishing the two 23S rRNA fragmentation sites in *R. leguminosarum* ATCC 10004^T suggest that different mechanisms are involved in their processing.

The existence of these two very different 23S rRNA fragmentation sites in *R. leguminosarum* ATCC 10004^T and in many other rhizobial and agrobacterial strains raises again the question about their physiological function. In addition to the 23S rRNA processing in domain III of *Rhizobiaceae*, only one case of rRNA fragmentation without involvement of IVSs was described until now, in the coccoid form (or the stationary-phase form) of *Helicobacter pylori* prior to rRNA degradation (20). In contrast to the situation in *H. pylori*, domain III processing in *R. leguminosarum* takes place during exponential growth and therefore does not directly initiate rRNA degradation. Unlike in *Salmonella* spp., cultures which quickly degrade their fragmented 23S rRNA as the cells enter the stationary phase (14), we did not observe strong 23S rRNA degradation during the stationary phase of *R. leguminosarum* cultures (monitored up to 60 h after inoculation; not shown). Thus, there is no obvious link between 23S rRNA fragmentation and its degradation in *R. leguminosarum*.

The function of ribosomes in protein synthesis is essential. Nevertheless, our knowledge about the rRNA processing steps required for ribosome biogenesis and the role of rRNA processing in ribosome turnover is poor. In this respect, elucidation of the mechanisms leading to the processing of helix 10 and domain III of 23S rRNA which is typical for many rhizobial strains will substantially add to our knowledge on this topic. Additionally, the unraveling of the mechanisms responsible for the changes in the amount of different rRNA fragments during growth of *R. leguminosarum* ATCC 10004^T cultures may contribute to our understanding of the regulation of ribosome concentration at different growth stages.

ACKNOWLEDGMENTS

We thank C. Conrad for providing purified RNases III, for reading the manuscript, and for help with the computing programs. We are grateful to A. Treuner-Lange and M. K. Ray for valuable comments. N. Amarger (INRA-CMSE, Dijon, France) and D. K. Jones (USDA/ARS Beltsville Rhizobium Germplasm Collection) provided rhizobial strains.

This work was supported by the Fonds der Chemischen Industrie and the Justus-Liebig-Universität Giessen (ATG71-56001041).

REFERENCES

1. **Amarger, N., V. Macheret, and G. Laguerre.** 1997. *Rhizobium gallicum* sp. nov. and *Rhizobium giardinii* sp. nov., from *Phaseolus vulgaris* nodules. Int. J. Syst. Bacteriol. **47:**996–1006.
2. **Ausubel, F. M., R. Brent, R. E. Kingston, D. D. Moore, J. G. Seidman, J. A. Smith, and K. Struhl.** 1989. Current protocols in molecular biology, vol. I. Greene Publishing Associates and Wiley-Interscience, New York, N.Y.
3. **Beringer, J. E.** 1974. R-factor transfer in *Rhizobium leguminosarum*. J. Gen. Microbiol. **84:**188–198.
4. **Bessarab, D. A., V. R. Kaberdin, C. L. Wei, G. G. Liou, and S. Lin-Chao.** 1998. RNA components of *Escherichia coli* degradosome: evidence for rRNA decay. Proc. Natl. Acad. Sci. USA **95:**3157–3161.
5. **Burgin, A. B., K. Parodos, D. J. Lane, and N. R. Pace.** 1990. The excision of intervening sequences from *Salmonella* 23S ribosomal RNA. Cell **60:**405–414.
6. **Christensen, H., S. Nordentoft, and J. E. Olsen.** 1998. Phylogenetic relationships of *Salmonella* based on rRNA sequences. Int. J. Syst. Bacteriol. **48:**605–610.
7. **Conrad, C., R. Rauhut, and G. Klug.** 1998. Different cleavage specifities of RNases III from *Rhodobacter capsulatus* and *Escherichia coli*. Nucleic Acids Res. **26:**4446–4453.
8. **Dryden, S. C., and S. Kaplan.** 1990. Localization and structural analysis of the ribosomal RNA operons of *Rhodobacter sphaeroides*. Nucleic Acids Res. **18:**7267–7277.
9. **Evguenieva-Hackenberg, E., and G. Klug.** 2000. RNase III processing of intervening sequences found in helix 9 of 23S rRNA in alpha-*Proteobacteria*. J. Bacteriol. **182:**4719–4729.
10. **Gerbi, S. A.** 1996. Expansion segments: regions of variable size that interrupt the universal core secondary structure of ribosomal RNA, p. 71–87. *In* R. A. Zimmermann and A. E. Dahlberg (ed.), Ribosomal RNA—structure, evolution, processing and function in protein biosynthesis. CRC Press, New York, N.Y.
11. **Gray, M. W., and M. N. Schnare.** 1996. Evolution of rRNA gene organization, p. 49–69. *In* R. A. Zimmermann and A. E. Dahlberg (ed.), Ribosomal RNA—structure, evolution, processing and function in protein biosynthesis. CRC Press, New York, N.Y.
12. **Gregory, S. T., M. O'Connor, and A. E. Dahlberg.** 1996. Functional *Escherichia coli* 23S rRNAs containing processed and unprocessed intervening sequences from *Salmonella typhimurium*. Nucleic Acids Res. **24:**4918–4923.
13. **Heck, C., A. Balzer, O. Fuhrmann, and G. Klug.** 2000. Initial events in the degradation of the polycistronic puf mRNA in *Rhodobacter capsulatus* and consequences for further processing steps. Mol. Microbiol. **35:**90–100.
14. **Hsu, D., L. M. Shih, and Y. C. Zee.** 1994. Degradation of rRNA in *Salmonella* strains: a novel mechanism to regulate the concentrations of rRNA and ribosomes. J. Bacteriol. **176:**4761–4765.
15. **Kordes, E., S. Jock, J. Fritsch, F. Bosch, and G. Klug.** 1994. Cloning of a gene involved in rRNA precursor processing and 23S rRNA cleavage in *Rhodobacter capsulatus*. J. Bacteriol. **176:**1121–1127.
16. **Ludwig, W., and K. H. Schleifer.** 1994. Bacterial phylogeny based on 16S and 23S rRNA sequence analysis. FEMS Microbiol Rev. **15:**155–173.
17. **Mattatall, N. R., and K. E. Sanderson.** 1998. RNase III deficient *Salmonella typhimurium* LT2 contains intervening sequences (IVSs) in its 23S rRNA. FEMS Microbiol Lett. **159:**179–185.
18. **Mathews, D. H., J. Sabina, M. Zuker, and D. H. Turner.** 1999. Expanded sequence dependence of thermodynamic parameters provides robust prediction of RNA secondary structure. J. Mol. Biol. **288:**911–940.
19. **Miller, W. L., K. Pabbaraju, and K. E. Sanderson.** 2000. Fragmentation of 23S rRNA in strains of *Proteus* and *Providencia* results from intervening sequences in the *rrn* (rRNA) genes. J. Bacteriol. **182:**1109–1117.
20. **Monstein, H. J., A. Tiveljung, and J. Jonasson.** 1998. Non-random fragmentation of ribosomal RNA in *Helicobacter pylori* during conversion to coccoid form. FEMS Immunol. Med. Microbiol. **22:**217–724.
21. **Nicolson, A. W.** 1999. Function, mechanism and regulation of bacterial ribonucleases. FEMS Microbiol. Rev. **23:**371–390.
22. **Pabbaraju, K., and K. E. Sanderson.** 2000. Sequence diversity of intervening sequences (IVSs) in the 23S ribosomal RNA in Salmonella spp. Gene **253**: 55–66.
23. **Pabbaraju, K., W. L. Miller, and K. E. Sanderson.** 2000. Distribution of intervening sequences in the genes for 23S rRNA and rRNA fragmentation among strains of the *Salmonella* reference collection B (SARB) and SARC sets. J. Bacteriol. **182:**1923–1929.
24. **Ralph, D., and M. McClelland.** 1993. Intervening sequence with conserved open reading frame in eubacterial 23S rRNA genes. Proc. Natl. Acad. Sci. USA **90:**6864–6868.
25. **Rauhut, R., A. Jäger, C. Conrad, and G. Klug.** 1996. Identification and analysis of the *rnc* gene for RNase III in *Rhodobacter capsulatus*. Nucleic Acids Res. **24:**1246–1251.
26. **Sambrook, J., E. F. Fritsch, and T. Maniatis.** 1989. Molecular cloning: a laboratory manual. Cold Spring Harbor Laboratory, Cold Spring Harbor, N.Y.
27. **Selenska-Pobell, S., and E. Evguenieva-Hackenberg.** 1995. Fragmentations of the large-subunit rRNA in the family *Rhizobiaceae*. J. Bacteriol. **177:**6993–6998.
28. **Selenska-Pobell, S., H. Döring, and E. Evguenieva-Hackenberg.** 1996. Unusual organization of the 23S rRNA genes in *Rhizobiaceae*. Soil Biol. Biochem. **29:**905–909.
29. **Selenska-Pobell, S., and H. Döring.** 1998. Sequences around the fragmentation sites of the large subunit ribosomal rRNA in the family *Rhizobiaceae*. Antonie van Leeuwenhoek **73:**55–67.
30. **Sterner, J. P., and M. A. Parker.** 1999. Diversity and relationships of bradyrhizobia from *Amphicarpaea bracteata* based on partial nod and ribosomal sequences. Syst. Appl. Microbiol. **22:**387–392.

31. **Tesfaye, M., D. J. Peterson, and F. B. Holl.** 1997. Comparison of partial 23S rDNA sequences from *Rhizobium* species. Can. J. Microbiol. **43:**526–533.
32. **Trust, T. J., S. M. Logan, C. E. Gustafson, P. J. Romaniuk, N. W. Kim, V. L. Chan, M. A. Ragan, P. Guerry, and R. R. Gutell.** 1994. Phylogenetic and molecular characterization of a 23S rRNA gene positions the genus *Campylobacter* in the epsilon subdivision of the Proteobacteria and shows that the presence of transcribed spacers is common in *Campylobacter* spp. J. Bacteriol. **176:**4597–4609.
33. **von Gabain, A., J. G. Belasco, J. L. Schottel, A. C. Y. Chang, and S. N. Cohen.** 1983. Decay of mRNA in *Escherichia coli*: investigation of the fate of specific segments of transcripts. Proc. Natl. Acad. Sci. USA **80:**653–657.
34. **Zahn, K., M. Inui, and H. Yukawa.** 1999. Characterization of a separate small domain derived from the 5′ end of 23S rRNA of an α-proteobacterium. Nucleic Acids Res. **27:**4241–4250.
35. **Zahn, K., M. Inui, and H. Yukawa.** 2000. Divergent mechanisms of 5′ 23S rRNA IVS processing in the alpha-proteobacteria. Nucleic Acids Res. **28:** 4623–4633.
36. **Zuker, M., D. H. Mathews, and D. H. Turner.** 1999. Algorithms and thermodynamics for RNA secondary structure prediction: a practical guide, p. 11–43. *In* J. Barciszewski and B. F. C. Clark (ed.), RNA biochemistry and biotechnology. NATO ASI Series. Kluwer Academic Publishers, Dordrecht, The Netherlands.